Design and evaluation of a novel solar-driven sustainable cogeneration system based on H_2O-LiBr working fluid.

J. A. Hernández Magallanes[1]*, D. De Santiago[1], Salvador Tututi-Ávila[1], Sanal K. C.[1].

[1] Faculty of Chemical Sciences, Autonomous University of Nuevo León, Monterrey (México)

Abstract

This study presents the theoretical design and simulation of an innovative absorption-based solar-assisted cogeneration cycle (SACC) that produces electricity in two stages by sequentially valorizing internally recovered waste heat. The proposed configuration integrates a Type III absorption heat pump in cascade with a regenerative Organic Rankine Cycle (ORC). Operated with low-temperature thermal sources, the system facilitates solar integration and clean energy utilization. Low-GWP working fluids are employed: H_2O–LiBr for the absorption subsystem and R-1233zd(E) for the ORC. Steady-state simulations were performed to assess the system's energy, exergy, and environmental performance, considering key parameters such as mass flow and pressure ratios, condensation temperatures (25–35 °C), and activation temperatures (120–190 °C)— ranges that are readily achievable with solar technologies such as evacuated tube, CPC, or parabolic trough collectors. At a refrigerant mass flow rate of 1 kg/s, the SACC delivers first- and second-stage power outputs of up to 1,400 kW and 3,400 kW, respectively, along with a thermal recovery of 10,904 kW ($\dot{Q}_A$) and exergy efficiencies of 0.67–0.70. The results confirm the feasibility of this sustainable alternative, which enhances waste-heat recovery, improves overall efficiency, and significantly reduces CO_2 emissions. Under equivalent operating conditions, the SACC achieves an estimated 40,583 metric tons of CO_2 reduction, compared with only 10,638 tons for the reference regenerative cycle (RRC or ORC). When normalized per unit of thermal energy supplied, the SACC attains 1.83 tCO_2eq per kW_{supply} avoided, whereas the RRC and ORC reach only 0.48–0.47 tCO_2eq per kW_{supply}, respectively—representing a 3.8-fold improvement in avoided emissions per unit of useful energy. Beyond its technical merits, the concept exhibits strong potential for hybrid solar-thermal applications in industrial and district energy systems, representing a promising pathway toward next-generation cogeneration technologies aligned with global decarbonization goals.

Keywords: Solar thermal energy, cogeneration systems, H_2O-LiBr absorption cycle, exergy efficiency, Sustainable Energy Conversion.

1. Introduction

The continuous growth of global energy demand represents a critical challenge for sustainable development and climate change mitigation. In 2024, worldwide final electricity consumption (IEA 2025) reached 27,400 TWh, of which a substantial share still originated from fossil fuels, with coal generation expanding by 1.3 % and natural gas generation by 1.9 % compared to 2023 (IEA 2023). According to the Global Carbon Project (2024), global carbon dioxide emissions from fossil fuels amounted to 37.4 Gt in 2024, marking a 0.8 % increase compared to 2023. Coal, oil, and natural gas were responsible for 41 %, 32 %, and 21 % of emissions, respectively, while the electricity and heat generation sector alone accounted for 45.5 % of the global total. These figures underscore the urgency of transitioning towards sustainable and low-carbon energy technologies.

Solar energy emerges as one of the most promising solutions to address these concerns. Meanwhile, the Solar Heat Worldwide (2025) report documented an operational solar thermal capacity of 544 GWth by the end of 2024, covering 777 million m² of collector area, delivering 443 TWh annually, and avoiding 153.5 million tons of CO_2 emissions. Importantly, solar thermal collectors cover a broad temperature spectrum: flat-plate and evacuated-tube collectors efficiently supply heat below 120 °C, whereas CPC and parabolic trough

10.18086/swc.2025.01.07 Available at http://proceedings.ises.org

collectors reach 150–400 °C, and central receiver or dish systems exceed 500 °C. This versatility makes solar thermal technologies ideally suited to activate advanced thermodynamic cycles operating with low-to-medium temperature sources.

Within this context, hybrid thermal cycles such as absorption systems, Organic Rankine Cycles (ORC), Kalina, and Goswami cycles have demonstrated strong potential for polygeneration and cogeneration applications. Several studies highlight their performance when integrated with renewable sources: Hashemian and Noorpoor (2019) developed a solar–biomass multigeneration system achieving 82.4 % energy efficiency and producing electricity, heating, cooling, hydrogen, and potable water. Chen et al. (2021) carried out the thermodynamic performance analysis and multi-criteria optimization of a hybrid CHP system integrated with a geothermal heat pump and natural gas. The study aimed to improve the system efficiency, reduce greenhouse gas emissions, and optimize energy, economic, and environmental performance, finding that the system achieved an energy saving ratio up to 30.24%, a carbon dioxide emission reduction ratio of 53.2%, and an annual cost saving ratio of 40.8%. More recently, Alharthi et al. (2023) reported solar-based combined energy systems reaching first-law efficiencies up to 72 % and second-law efficiencies of 25 %. Zhang (2024) explored the integration of combined-cycle power plants (CCPPs) with renewable energy sources (solar), to create hybrid systems for sustainable energy solutions. It has been proven that integrating renewable energy with CCPPs enhances operational flexibility, reduces greenhouse gas emissions, and improves grid stability. Liu et al. (2023) investigated a novel CHP system integrated with solar energy to address the limitations of traditional CHP systems in efficiency and flexibility. The energy, exergy, and operational flexibility of the system were analyzed using a 330 MW unit as a base-case. In such conditions, the system achieved an energy efficiency of 54.7% during daytime and 55.8% at nighttime, surpassing traditional CHP systems, and saving up to 295.35 tons of coal per day during the heating season.

Building on this research, the present study proposes and simulates an innovative absorption-based **solar-**assisted cogeneration cycle (SACC) capable of operating with low-temperature solar energy as the primary source, while retaining flexibility for other alternatives such as biomass, geothermal, or industrial waste heat. The system integrates a Type III absorption heat pump in cascade with a regenerative ORC, enabling sequential valorization of heat and maximizing electricity production. Low-GWP working fluids are employed to minimize environmental impacts, while performance is assessed through energy, exergy, and environmental indicators. By focusing on the synergy between solar thermal technologies and advanced thermodynamic cycles, this work seeks to demonstrate a feasible pathway for sustainable electricity generation and thermal recovery, contributing to global decarbonization efforts.

2. Proposal configuration and performance parameters

The solar-assisted cogeneration cycle (SACC) (Figure 1) integrates absorption and Rankine-based technologies to simultaneously generate electricity and recover useful heat. The configuration builds upon the base concept introduced by Hernández-Magallanes et al. (2022), which integrates a Type I Absorption Heat Pump (AHP) and a Type II Absorption Heat Transformer (AHT). In the present work, this configuration is extended with the inclusion of a regenerative Organic Rankine Cycle (ORC) to maximize the valorization of available thermal energy. The system operates with two thermal generators at different activation levels: a high-temperature generator (T_{HG}, 120–190 °C) and a low-temperature generator (T_{LG}, 80 °C). The T_{HG} provides a high-enthalpy working fluid that drives Turbine 1, producing mechanical work that is converted into electricity. In parallel, the T_{LG} recovers and upgrades heat released during the exothermic absorption process, enabling further refrigerant desorption and strengthening the thermal cascade. In both thermal generators, solar energy can serve as the primary activation source, with different solar collector technologies employed according to the operating ranges. Alternatively, hybrid sources such as biomass or residual heat can also be utilized, increasing system flexibility and reliability. The integration of the regenerative ORC allows additional conversion of the recovered absorber heat into electricity, thereby increasing the overall power output and improving system efficiency. By operating across three pressure levels and two activation temperature sources, the configuration ensures compatibility with solar thermal collectors and other renewable or low-grade heat sources. This arrangement highlights the potential of absorption–ORC hybridization as a sustainable cogeneration strategy, capable of enhancing energy efficiency, valorizing low-to-medium temperature heat, and contributing to greenhouse gas mitigation.

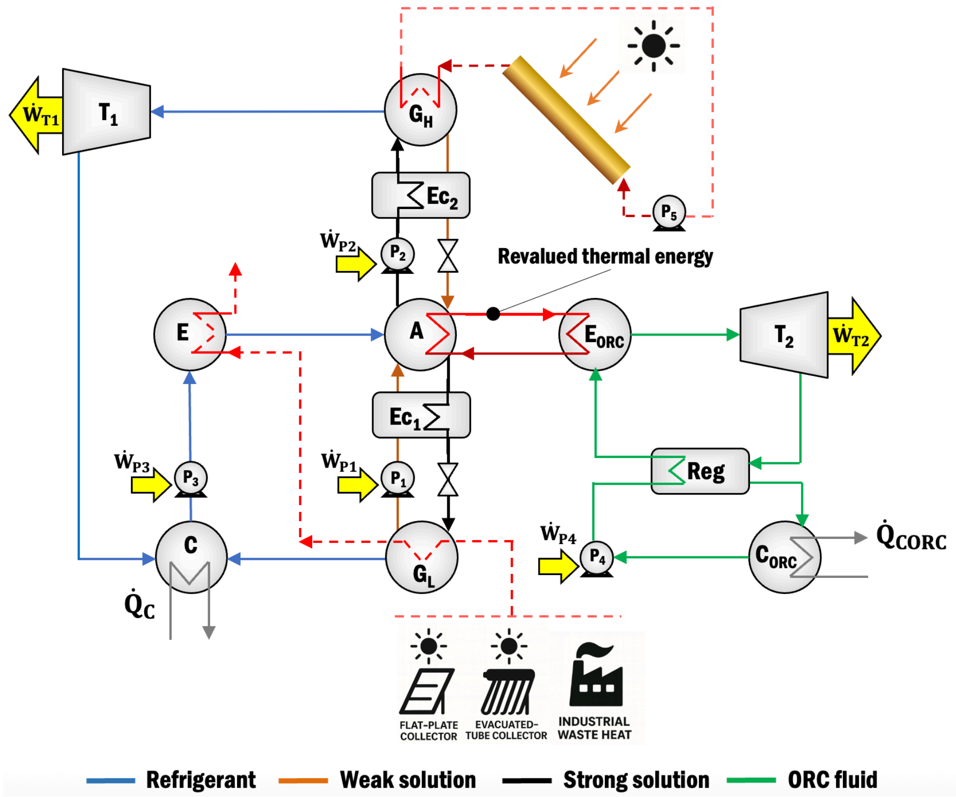

Figure 1: The SACC, integrating AHP, AHT, and a regenerative ORC, operating with two activation levels (T_{HG}: 120–160 °C; T_{LG}: 80 °C) to maximize electricity generation and thermal recovery from low-to-medium temperature sources.

The thermodynamic model of the proposed cogeneration system was developed and solved using Engineering Equation Solver (EES). Mass and energy balances were established for each component, following the methodology introduced by Dereje et al. (2015), and extended here to integrate the hybrid absorption–ORC configuration. The thermophysical properties of the working fluids (H_2O–LiBr for the absorption-based cycles and R-1233zd(E) (Eyerer et al. 2016) for the ORC) were determined under steady-state operation. This enabled a complete thermodynamic characterization of the system under different operating conditions.

For the analysis of the processes, a set of key thermodynamic variables was considered. These include the high-temperature source (T_{HG}), the low-temperature source (T_{LG}), the condensation temperature (T_C), the pressure ratio (PR), the mass flow ratio (MFR), and the thermal recovery temperature or Gross Temperature Lift (GTL). The influence of each parameter on system performance is examined, while their operating ranges are discussed in a subsequent section. The following assumptions were applied in the modeling:

(i) the system operates under steady-state and thermodynamic equilibrium conditions;

(ii) pressure drops in pipes and components were neglected, except in expansion valves;

(iii) expansion processes in valves were assumed isoenthalpic;

(iv) saturated states were assumed at the outlets of condensers and evaporators;

(v) heat losses to the environment were neglected;

(vi) changes in kinetic and potential energy were considered negligible;

(vii) the thermal efficiency of the regenerator was fixed at 0.70 (Hernández-Magallanes et al. 2022);

(viii) the isentropic efficiencies of the turbine and the pump were set to 0.88 (López-Villada et al. 2014) and 0.80 (Vijayaraghavan, 2003), respectively.

The governing equations are expressed as follows. The steady-state mass balance for each control volume is:

$$\sum \dot{m}_i = \sum \dot{m}_o \quad \text{(eq. 1)}$$

The energy balance is written as:

$$\sum \dot{m}_i h_i - \sum \dot{m}_o h_o + \dot{Q} - \dot{W} = 0 \quad \text{(eq. 2)}$$

where $\dot{m}$ represents the mass flow rate (kg·s^{-1}); $\dot{Q}$ the thermal load (kW); $\dot{W}$ the mechanical power output (kW); and h the specific enthalpy (kJ·kg^{-1}). Subscripts i and o refer to inlet and outlet conditions, respectively.

The net work output of the system is obtained from the turbine and pump contributions:

$$\dot{W}_{net} = \dot{W}_{T1} + \dot{W}_{T2} - \dot{W}_{b1} - \dot{W}_{b2} - \dot{W}_{b3} - \dot{W}_{b4} \quad \text{(eq. 3)}$$

To assess system performance, two parameters are considered: the effective first-law efficiency (η_I) and the exergy efficiency (η_{Ex}). The first law does not account for heat quality, and thus it cannot capture losses due to irreversibilities. To prevent overestimating efficiency by ignoring the quality of recovered heat ($\dot{Q}_A$), the effective first-law efficiency, Vijayaraghavan and Goswami (2003), is defined in eq. 4:

The effective first-law efficiency ($\eta_{I,eff}$) is defined as:

$$\eta_I = \frac{\text{Main products (produced energy)}}{\text{Thermal inputs (activation energy)}} = \frac{\dot{W}_{net}}{\dot{Q}_{HG}+\dot{Q}_{LG}+\dot{Q}_E} \quad \text{(eq. 4)}$$

For its part, an appropriate thermodynamically consistent method is to consider the exergy associated with the upgraded heat output ($\dot{Q}_A$) and heat inputs. Therefore, exergy efficiency measures the fraction of exergy that enters the cycle and leaves as useful output (Hernández-Magallanes et al. 2022), as shown in eq. 5:

The exergy efficiency (η_{Ex}) is defined as:

$$\eta_{Ex} = \frac{\dot{W}_{net}}{\sum \dot{Q}_{SUM}} \quad \text{(eq. 5)}$$

Where, the thermal input supplied to the cycle is given by:

$$\sum \dot{Q}_{SUM} = \dot{Q}_{HG}\left(1 - \frac{TK_0}{TK_{HG}}\right) + \dot{Q}_{LG}\left(1 - \frac{TK_0}{TK_{LG}}\right) + \dot{Q}_E\left(1 - \frac{TK_0}{TK_E}\right) \quad \text{(eq. 6)}$$

where temperatures are absolute, and TK_o represents the heat sink temperature.

3. Results

This section summarizes the key findings obtained from the simulation of the SACC. The evaluation was carried out by varying the main operating parameters within representative ranges: condensation temperature (T_C = 25–35 °C), low-temperature activation source (T_{LG} = 80 °C), high-temperature activation source (T_{HG} = 100–190 °C), and absorption temperature (constrained between $T_{LG} < T_A < T_{HG}$). In addition, parametric analyses were performed for pressure ratio (PR = 3) and mass flow rate ratio (MFR = 3). These ranges were selected to reflect realistic operating conditions of solar thermal collectors and other renewable or low-grade heat sources, ensuring consistency with the assumptions outlined in the methodology.

3.1 Net power output

The SACC is designed to generate electricity through two subsystems: the primary absorption-based cycle and the secondary regenerative ORC. Figure 2 illustrates the net power output ($\dot{W}_{Net}$) as a function of the thermal recovery temperature (GTL), highlighting the individual contributions of both subsystems. As shown, the power produced by the primary turbine ($\dot{W}_{Net1}$) remains essentially constant under the evaluated conditions, since it is directly defined by the high-temperature source (T_{HG} = 160 °C), the condensation temperature (T_C = 30 °C), and the fixed pressure ratio (PR = 3). In this case, the first turbine produces up to 1,400 kW, establishing a baseline level of power generation that is insensitive to variations in GTL. In contrast, the secondary turbine of the ORC ($\dot{W}_{Net2}$) exhibits a strong dependence on the revalorized heat supplied by the primary absorption system. As the recovery temperature (GTL) increases, the available thermal potential grows, leading to a gradual rise in the power output of the ORC. For intermediate values of GTL, the secondary contribution reaches approximately 3,000 kW, while at higher GTL levels the output increases sharply, achieving up to 4,500 kW. This behavior demonstrates the high potential of the hybrid configuration to improve electricity production under identical boundary conditions. While the absorption-based cycle ensures stable baseline generation, the integration of the ORC allows for significant performance enhancement by exploiting revalorized heat, thus confirming the advantages of the proposed solar-assisted cogeneration system.

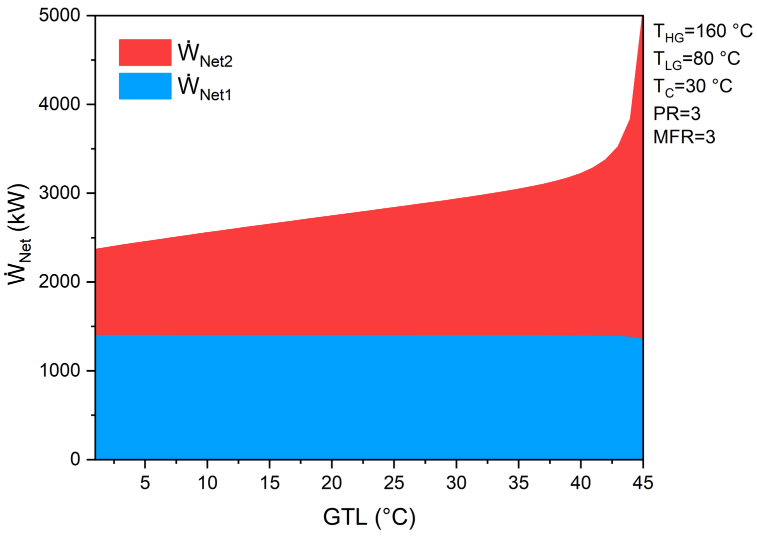

Figure 2. Net power output ($\dot{W}_{Net}$) of the SACC, showing the individual contributions from the absorption system ($\dot{W}_{Net1}$) and the ORC ($\dot{W}_{Net2}$).

3.2 Exergy Efficiency Analysis

The exergy efficiency (η_{Ex}) of the SACC was evaluated as a function of the condensation temperature (T_C), high-temperature source (T_{HG}), and thermal recovery temperature (GTL). Figure 3 presents the results for three representative cases: (a) T_C = 25 °C, (b) T_C = 30 °C y (c) T_C = 35 °C. Overall, the system achieves a maximun exergy efficiencies in the range of 0.67–0.70. These values highlight the good thermodynamic performance of the configuration, although a slight reduction in efficiency is observed as the condensation temperature increases. As the condensation temperature increases, the span of revalued (or recovered) temperature levels progressively decreases — from 65 °C in the GTL condition to 59 °C and finally to 51 °C under the established condensation temperatures (T_C). This trend indicates a reduced thermal potential available for recovery at higher condensation levels. This trend is consistent with the higher irreversibilities introduced at elevated T_C, which reduce the available temperature gradient for heat transfer. The inclusion of the ORC introduces additional irreversibilities, primarily due to the transfer of recovered heat (Q_A) to the R1233zd(E) refrigerant and its subsequent expansion. As a result, a marginal decrease in exergy efficiency is noted. However, this compromise is offset by a substantial improvement in net power generation, with the hybrid configuration producing up to 2.2 times more electricity than the absorption cycle alone. These results confirm that while exergy efficiency is slightly penalized by the hybridization process, the trade-off is favorable when considering global performance. The solar-assisted cogeneration configuration significantly enhances electricity output while maintaining competitive efficiency levels, reinforcing its potential as a sustainable solar-based cogeneration strategy.

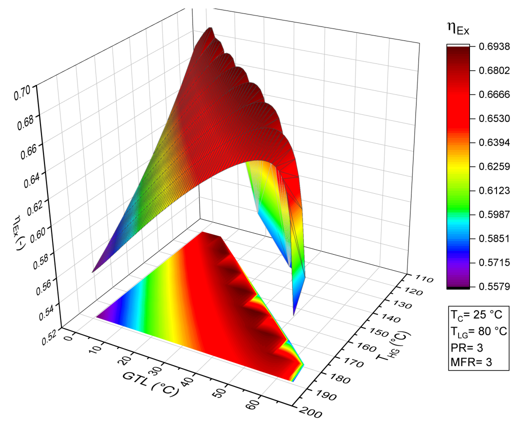

a)

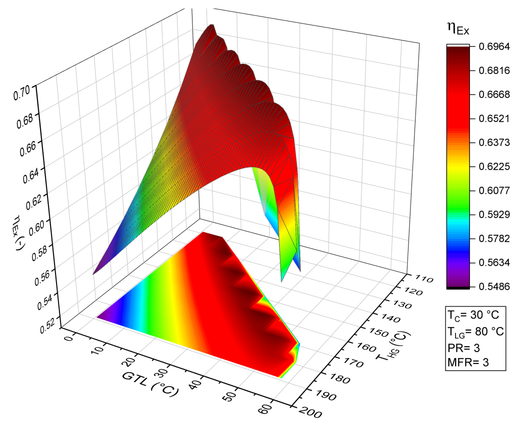

b)

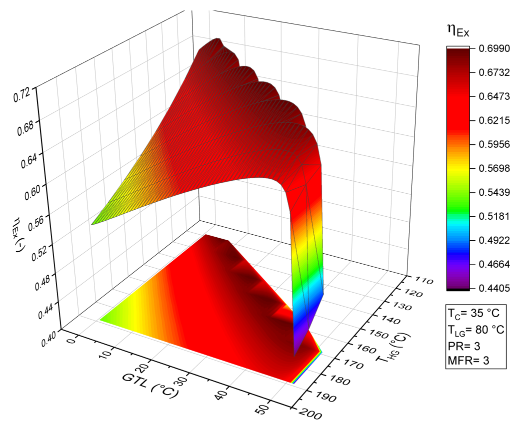

c)

Figure 3: Exergy efficiency (η_{Ex}) of the SACC as a function of T_{HG} and GTL for different condensation temperatures: (a) T_C = 25 °C, (b) T_C = 30 °C, and (c) T_C = 35 °C.

3.3 First-Law Efficiency Analysis

The first-law efficiency (η_I) of the SACC was evaluated for different condensation temperatures (T_C) and activation conditions, as illustrated in Figure 4. The results show that in the SACC (absorption system + ORC), the efficiency values progressively decrease, reaching stable maximum values of approximately 0.17, 0.16, and 0.14 for T_C = 25, 30, and 35 °C, respectively. In contrast, the reference Cycle I (absorption system only) presents slightly higher values for the same condensation temperatures (Hernández-Magallanes et al. 2022). This comparison indicates that the exclusion of the direct thermal contribution in hybrid Cycle leads to a measurable reduction in first-law efficiency. The result is consistent with the additional irreversibilities introduced by the ORC integration and the redistribution of recovered heat, which prioritize electricity generation over thermal recovery.

Another relevant observation concerns the operational limits of the system at elevated thermal recovery temperatures (GTL). As shown in Figures 4a–c, for a given condensation temperature, the upper GTL limit depends largely on the high thermal activation source. As this source is reduced, the operating window for heat recovery potential also narrows, and thus the GTL decreases (which translates to a lower potential for the secondary circuit). This behavior reflects the greater thermal constraints imposed at higher condensation temperatures, which modify the cycle's effective operating window.

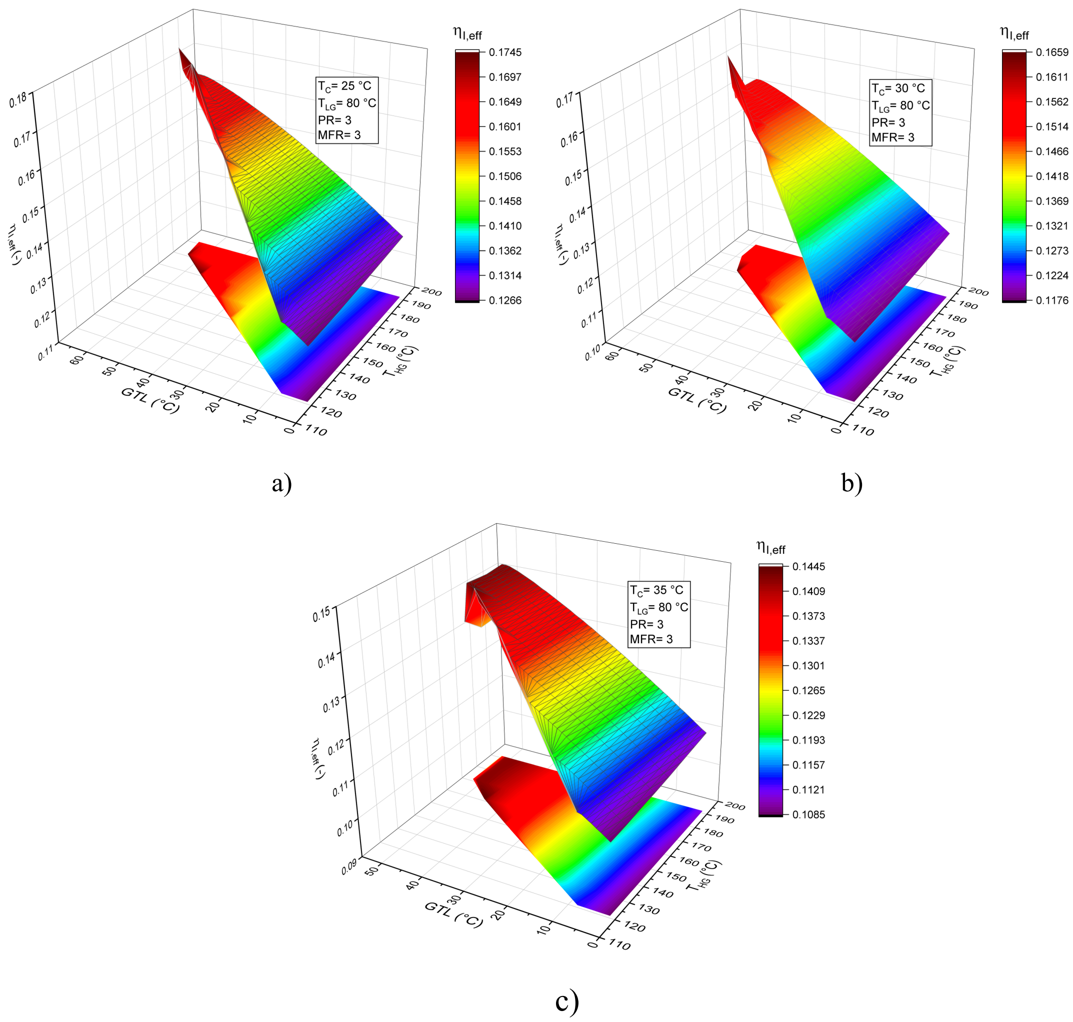

Figure 4. First-law efficiency (η_I) of the SACC as a function of T_{HG} and GTL for different condensation temperatures: a) T_C = 25 °C, b) T_C = 30 °C, c) T_C = 35 °C.

3.4 Avoided Emissions Analysis

Regarding the potential for avoided emissions, the SACC configuration demonstrates a significant environmental benefit due to the higher electricity generation compared to the baseline absorption cycle. Assuming that the system is activated by renewable heat sources, the increase in power output directly translates into higher levels of carbon dioxide equivalent (tCO_2e) avoided.

As shown in Figure 5, the maximum average avoided emissions reach 38,667, 37,482, and 35,629 tCO_2e per year for condensation temperatures of T_C = 25, 30, and 35 °C, respectively. These values exceed those obtained with the baseline cycle by an average margin of approximately 12 % (Hernández-Magallanes et al. 2022). The trend also shows that as the condensation temperature increases; the environmental benefits are slightly reduced due to the decline in both efficiency and power generation potential.

It is also worth noting that, although there are very small regions where the avoided emissions could be even higher, these occur near the crystallization boundary of the working pair. Consequently, they do not represent feasible operating conditions for the cycle and are excluded from the viable performance envelope.

Overall, these results confirm that it is possible to expand electricity production at relatively low operating temperatures without compromising the environmental objective of reducing carbon emissions. The hybrid cogeneration system therefore reinforces its viability not only from a thermodynamic standpoint but also from an environmental perspective, underscoring its role as a sustainable pathway for clean energy integration.

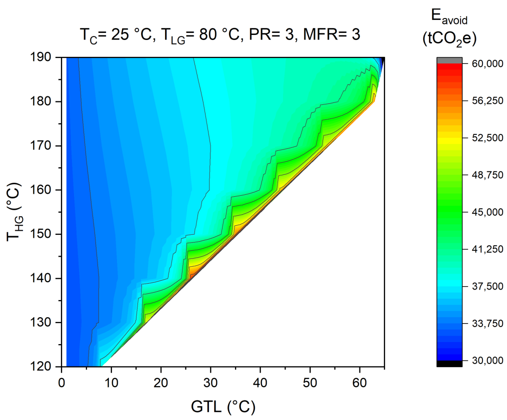

a)

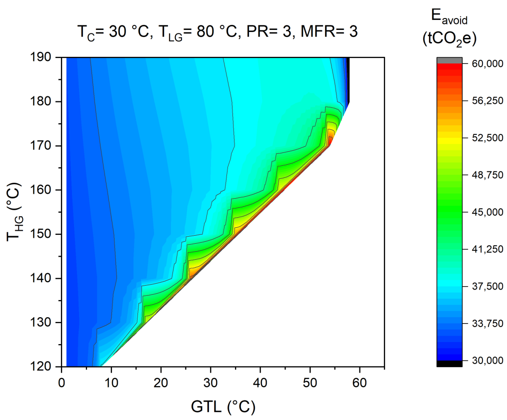

b)

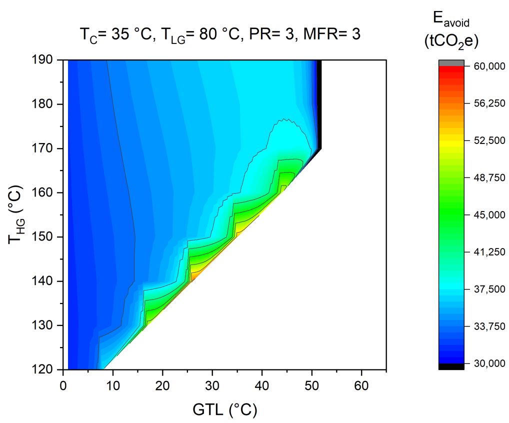

c)

Figure 5. Annual avoided emissions (tCO_2e) of the SACC as a function of T_{HG} and GTL for different condensation temperatures: a) T_C = 25 °C, b) T_C = 30 °C, c) T_C = 35 °C.

3.5 Comparative Case Study and Closing Remarks

To strengthen the discussion, a comparative case study was carried out under equivalent operating conditions for the SACC and two conventional electricity generation systems: a regenerative Rankine cycle (RRC) and a conventional Organic Rankine Cycle (ORC). The operating conditions and performance indicators are summarized in Table 1 and Table 2, respectively, where Q_{supply} denotes the thermal energy supplied to the cycle, and $Q_{rejected}$ represents the rejected heat dissipated to the environment.

Table 1. Operating conditions of the thermodynamic cycles under equivalent working conditions.

Operating conditions	Case study	Unit
T_C	30	°C
T_{HG}	160	°C
$T_{LG} = T_E$	80	°C
T_A	120	°C
RP	3	-
RF	3	-
$\dot{m}_{R\_LG}$ (calculation base)	1	kg/s

Table 2. Performance parameters of the thermodynamic cycles under equivalent operating conditions.

Parameter	SACC (absorption system + ORC)	Conventional RRC	Conventional ORC
Working fluid	1. H_2O-LiBr 2. R1233zd(E)	H_2O	n-Pentano
$\dot{W}_{Net}$ (kW)	3,220 (15%)	3,868 (18%)	3,777 (17%)
$\dot{Q}_{Rejected}$ (kW)	18,836 (85%)	18,188 (82%)	18,279 (83%)
$\dot{Q}_{Supply}$ (kW)	22,056 (100%)	22,056 (100%)	22,056 (100%)
CO_2 (tCO_2e)	40,583	10,638	10,388
η_I	0.146	0.175	0.171
η_{Ex}	0.696	0.584	0.748

The results confirm that the SACC, designed to utilize both direct solar thermal input and revalorized heat from the absorption subsystem, attains a first-law efficiency ($\eta_I = 0.146$) approximately 16 % lowerthan that of the CRR and ORC reference systems. This reduction is mainly attributed to the greater thermal input demanded by the absorption stages.

However, when assessed in terms of exergy efficiency, the SACC exhibits a superior performance compared with the CRR (0.696 vs. 0.584) and approaches that of the ORC (0.748). It is also noteworthy that the refrigerant employed in the ORC section of the hybrid configuration shows lower thermal performance but considerably improved environmental characteristics.

Regarding thermal-to-electricity conversion, the SACC reaches a direct conversion efficiency of about 15 %, compared with 17–18 % for the conventional cycles. Nonetheless, this configuration benefits from the additional power generated through the recovery of absorption heat, partially compensating for its lower first-law efficiency.

From an environmental standpoint, the absolute CO_2 emissions of the SACC are higher than those of the standalone CRR and ORC, as it incorporates a second turbine to maximize power output. Yet, when normalized per unit of thermal energy supplied, the SACC achieves 1.83 tCO_2eq per kW_{supply} avoided, compared with only 0.48–0.47 tCO_2eq per kW_{supply} for the CRR and ORC, respectively. This represents a 3.8-

fold increase in avoided emissions per unit of useful energy—an appreciable improvement under sustainability criteria.

Furthermore, the adoption of the low-GWP refrigerant R-1233zd(E) in the ORC section further strengthens the environmental profile of the proposed configuration relative to conventional ORCs employing n-pentane. The system also stands out for its capacity to reuse residual heat from the absorption subsystem, thereby reducing the demand for external thermal input.

In summary, despite its slightly lower first-law efficiency, the solar-assisted cogeneration cycle demonstrates competitive exergy performance coupled with a marked reduction in carbon emissions per unit of energy supplied. These results position it as an energetically viable and environmentally advantageous alternative, particularly suitable for applications harnessing solar or low-grade thermal energy sources.

4. Conclusions

The SACC demonstrates strong potential as a sustainable alternative for low-grade thermal energy conversion. Under the evaluated operating conditions, the system achieves net power outputs exceeding 3.2 MW by combining the absorption-based section with an integrated regenerative ORC, while maintaining exergy efficiencies between 0.67 and 0.70. Although its first-law efficiency (≈15 %) is lower than that of conventional cycles (≈17–18 %), this drawback is compensated by the ability to reuse recovered heat, effectively maximizing the utilization of the supplied energy.

From an environmental standpoint, the cycle offers a substantial advantage. Normalized avoided emissions reach up to 1.83 tCO_2eq per kW_{supply}, approximately 3.8 times higher than conventional CRR and ORC configurations. This performance is reinforced using low-GWP refrigerant R1233zd(E) in the ORC section, positioning the system as both technologically and environmentally robust.

The parametric study highlights that the most influential operating variables are the activation temperatures (T_{HG} and GTL), condensation temperature (T_C), and pressure ratio (PR). These parameters define the feasible envelope by balancing thermal recovery, crystallization risk, and turbine performance. Careful selection of these ranges is critical to ensure efficient operation while avoiding excessive irreversibilities.

Overall, the results confirm that the solar-assisted cogeneration cycle can significantly enhance electricity production and emission reduction compared to conventional systems, even when operating with relatively low-temperature inputs. This positions it as a viable and scalable pathway for integrating solar energy and other renewable or residual heat sources into future clean energy strategies.

5. Acknowledgments

The author gratefully acknowledges the Facultad de Ciencias Químicas of the Universidad Autónoma de Nuevo León (UANL, Mexico) for the institutional support that made it possible to participate in the Solar World Congress (SWC) 2025.

6. References

Alharthi, M. A., Khaliq, A., Alqaed, S., & Almehmadi, F. (2023). Investigation of new combined cooling, heating and power system based on solar thermal power and single-double-effect refrigeration cycle. Energy Reports, 9, 289–309.

Ayou, D., Bruno, J. C., & Coronas, A. (2015). Combined absorption power and refrigeration cycles using low- and mid-grade heat sources. Science and Technology for the Built Environment, 21, 934–943.

Chen, Y., Zhao, D., Xu, J., Wang, J., & Lund, P. (2021). Performance analysis and exergo-economic optimization of a solar-driven adjustable tri-generation system. Energy Conversion and Management, 233, 113873.

Eyerer, S., Wieland, C., Vandersickel, A., & Spliethoff, H. (2016). Experimental study of an ORC (Organic Rankine Cycle) and analysis of R1233zd-E as a drop-in replacement for R245fa for low temperature heat utilization. Energy, 103, 660–671.

Global Carbon Project. (2024). Fossil fuel CO_2 emissions increase again in 2024 (Revised on 25/09/2025). Retrieved from https://globalcarbonbudget.org/fossil-fuel-co2-emissions-increase-again-in-2024/

Hashemian, N., & Noorpoor, A. (2019). Assessment and multi-criteria optimization of a solar and biomass-based multi-generation system: Thermodynamic, exergoeconomic and exergoenvironmental aspects. Energy Conversion and Management, 195, 788–797.

Hernández-Magallanes, J. A., Domínguez-Inzunza, L., Lugo-Loredo, S., Sanal, K., Cerdán-Pasarán, A., Tututi-Avila, S., & Morales, L. (2022). Energy and exergy analysis of a modified absorption heat pump (MAHP) to produce electrical energy and revaluated heat. Processes, 10, 1–19.

International Energy Agency. (2025). Electricity Market Report: Mid-Year Update 2025 (Revised on 25/09/2025). Paris: IEA. Retrieved from https://www.iea.org/reports/electricity-mid-year-update-2025

International Energy Agency. (2023). Energy Statistics Data Browser – Total Electricity Consumption: Mexico. Paris: IEA. 2025 (Revised on 25/09/2025). https://www.iea.org/data-and-statistics/data-tools/energy-statistics-data-browser?country=MEXICO&fuel=Energy%20consumption&indicator=TotElecCons

Klein, S. A. (2015). Engineering Equation Solver (EES). Madison, USA: F-Chart Software.

Liu, R., Liu, M., Xu, C., Liu, M., & Yuan, W. (2023). Thermodynamic study of a novel combined heat and power system integrated with solar energy. Applied Thermal Engineering, 234, 121192.

López-Villada, J., Ayou, D., Bruno, J. C., & Coronas, A. (2014). Modelling, simulation and analysis of solar absorption power-cooling systems. International Journal of Refrigeration, 39, 125–136.

Vijayaraghavan, S., & Goswami, D. Y. (2003). On evaluating efficiency of a combined power and cooling cycle. Journal of Energy Resources Technology, Transactions of the ASME, 125, 221–227.

Weiss, W., & Spörk-Dür, M. (2025). Solar Heat Worldwide: Global Market Development and Trends in 2024. Detailed Market Figures 2023. IEA Solar Heating & Cooling Programme, AEE INTEC.

Zhang, Z. (2024). Combined cycle power plants and renewable energy integration – Hybrid systems for sustainable energy solutions. Highlights in Science, Engineering and Technology, 120, 586–591.